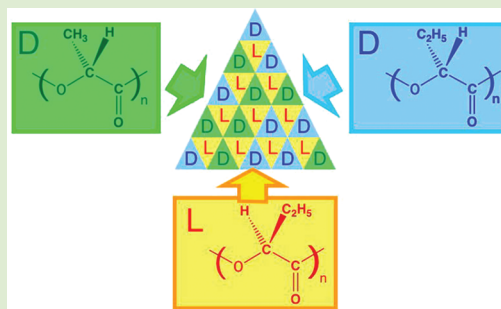


Ternary Stereocomplex Formation of One L-Configured and Two D-Configured Optically Active Polyesters, Poly(L-2-hydroxybutanoic acid), Poly(D-2-hydroxybutanoic acid), and Poly(D-lactic acid)

Hideto Tsuji,* Mao Hosokawa, and Yuzuru Sakamoto

Department of Environmental and Life Sciences, Graduate School of Engineering, Toyohashi University of Technology, Tempaku-cho, Toyohashi, Aichi 441-8580, Japan

ABSTRACT: The ternary stereocomplex formation of optically active polyesters, L-configured poly(L-2-hydroxybutanoic acid) [P(L-2HB)] and D-configured poly(D-2-hydroxybutanoic acid) [P(D-2HB)] and poly(D-lactic acid) (PDLA), is reported. Ternary P(L-2HB)/P(D-2HB)/PDLA blends were prepared by solution-casting to have a fixed content (50 mol %) of L-configured P(L-2HB) and different contents of D-configured P(D-2HB) relative to those of PDLA, and stereocomplex formation in the blends was investigated using wide-angle X-ray scattering and differential scanning calorimetry. The interplane distances of solution- and melt-crystallized blends were estimated from the 2θ values at around 11° and 22° , and the melting temperatures of stereocomplex increased continuously with increasing the P(D-2HB) content relative to that of PDLA in the blends, indicating the formation of a ternary stereocomplex. The stereocomplex crystallinity values of ternary blends were much higher than the values calculated from binary P(L-2HB)/P(D-2HB) and P(L-2HB)/PDLA blends wherein respectively only the binary P(L-2HB)/P(D-2HB) homostereocomplex and P(L-2HB)/PDLA heterostereocomplex were formed, reflecting the facile crystallization of the ternary stereocomplex.



Homostereocomplex (HMSC) formation is reported for enantiomeric L- and D-configured optically active biodegradable polyesters,^{1–4} such as poly(α -methyl- α -ethyl- β -propiolactone)s,⁵ poly(β -propiolactone)s with different side groups containing chlorides,⁶ poly(lactide)s [i.e., poly(lactic acid)s, PLAs, (O–CH(CH₃)–CO)_n],⁷ and poly(2-hydroxybutyrate) [i.e., poly(2-hydroxybutanoic acid)s, P(2HB)s, (O–CH(C₂H₅)–CO)_n].⁸ On the other hand, heterostereocomplex (HTSC) formation is found for PLA and P(2HB) with opposite configurations.^{9,10} The wide-angle X-ray scattering (WAXS) of HMSCs of enantiomeric PLAs and P(2HB)s and HTSC of PLA and P(2HB) strongly suggested that the lattice sizes decrease in the following order: HMSC of enantiomeric P(2HB)s > HTSC of P(2HB) and PLA > HMSC of enantiomeric PLAs.⁹

An intensive study has been carried out for the HMSCs of enantiomeric PLAs and P(2HB)s and found that mechanical and barrier properties, hydrolytic and thermal degradation-resistance can be improved and crystallization is accelerated by HMSC formation.^{1–4,11,12} HMSC formation occurs not only in polymer blends but also in stereoblock copolymers.^{1–4,10,13–15} Although it is favorable to use high molecular weight polymers for preparing high-performance PLA-based materials, HMSC formation of enantiomeric PLAs is limited in the polymer blends when the constituent polymers have molecular weights exceeding 10^5 g mol⁻¹, in marked contrast with stereoblock copolymers.^{1–4} Numerous methods were developed for polymer blending to overcome this issue. They include thermal

drawing^{16,17} and annealing,^{18–20} electrospinning,^{21–23} solution casting with solvent–nonsolvent mixture²⁴ or supercritical carbon dioxide,²⁵ and repeated solution casting.²⁶ More recently, Yang et al. reported a detailed formation mechanism of PLA HMSC at an early stage.²⁷

In the present study, we investigated the crystallization of ternary blends of poly(L-2-hydroxybutyrate) [i.e., poly(L-2-hydroxybutanoic acid), P(L-2HB)], poly(D-2-hydroxybutyrate) [i.e., poly(D-2-hydroxybutanoic acid), P(D-2HB)], and poly(D-lactic acid) (PDLA) having various polymer blend ratios using WAXS and differential scanning calorimetry (DSC) and herewith first report the ternary stereocomplex formation of L-configured P(L-2HB) and D-configured P(D-2HB) and PDLA at an arbitrary ratio of P(D-2HB) content to that of PDLA in the ternary blends. Moreover, as far as we are aware, this is the first report of the ternary crystal formation from three different crystalline polymers. Ternary stereocomplex formation is expected to open a new versatile way to prepare biodegradable materials having a wide variety of physical properties and biodegradability.

P(L-2HB), P(D-2HB), and PDLA were synthesized by the polycondensation of L- and D-2-hydroxybutanoic acids and ring-opening polymerization of D-lactide, respectively. Blends were prepared by solution casting (solution-crystallized samples) and

Received: April 1, 2012

Accepted: May 10, 2012

Published: May 17, 2012

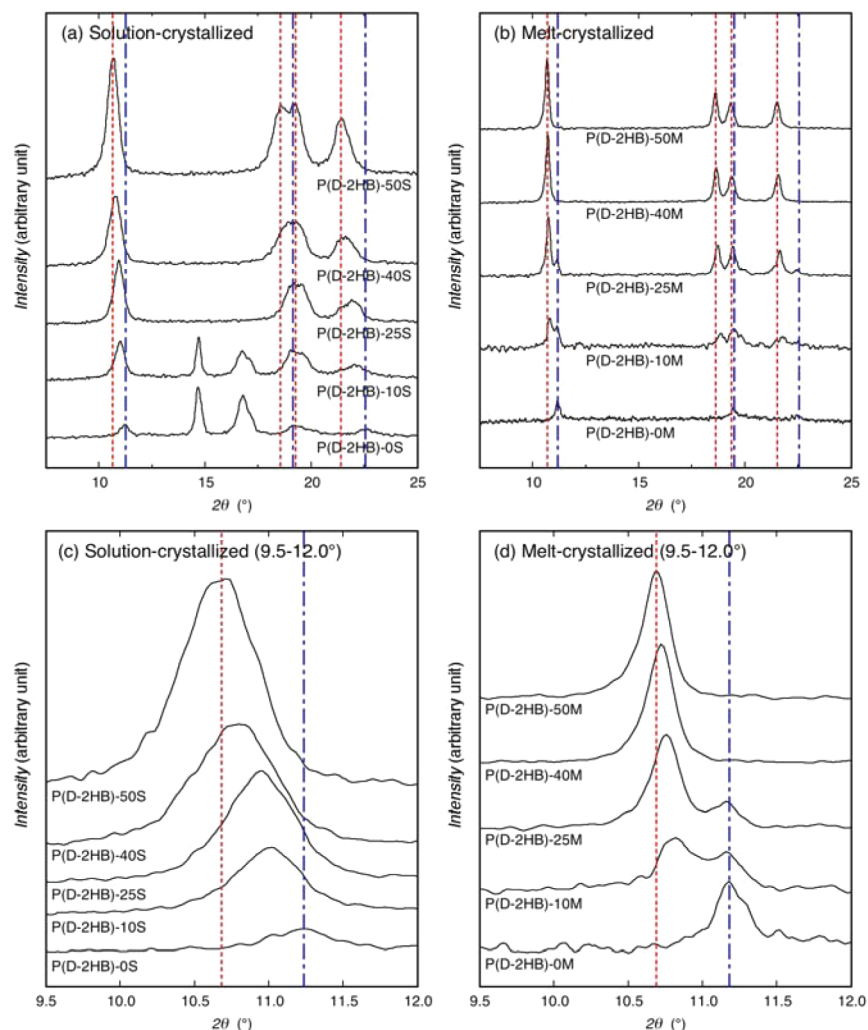


Figure 1. WAXS profiles of solution-crystallized (a,c) and melt-crystallized (b,d) blends. Parts c and d are magnified figures in the 2θ range of $9.5\text{--}12.0^\circ$ of parts a and b. Red and blue lines are crystalline diffraction peaks of P(L-2HB)/P(D-2HB) HMSC and P(L-2HB)/PDLA HTSC crystallites.

by melt-crystallization of the as-cast blends (melt-crystallized samples). For the estimation of crystalline species and crystallinity formed by different crystallization methods at different polymer blend ratios, WAXS measurements were performed. Figure 1 shows the WAXS profiles of the ternary P(L-2HB)/P(D-2HB)/PDLA blends at P(D-2HB) contents of 10–40 mol %, together with those of the reference binary P(L-2HB)/PDLA and P(L-2HB)/P(D-2HB) blends at P(D-2HB) contents of 0 and 50 mol %, respectively. Also, the magnified WAXS profiles in the 2θ range of $10.7\text{--}11.3^\circ$ are shown in parts c and d. In the present study, the blends are abbreviated as P(D-2HB)-XS(or M), where X is mol % of P(D-2HB) in the blend and S and M mean solution- and melt-crystallized, respectively. The P(L-2HB), P(D-2HB), and PDLA contents in a blend P(D-2HB)-X are 50, X, and $50\text{--}X$ mol %, respectively. For the binary solution-crystallized P(D-2HB)-50S and melt-crystallized P(D-2HB)-50M, only P(L-2HB)/P(D-2HB) HMSC crystalline diffraction peaks were observed at 2θ values around 10.7° , 18.6° (subpeak: 19.3°), and 21.5° .⁸ For the binary melt-crystallized P(D-2HB)-0M, only P(L-2HB)/PDLA HTSC crystalline diffraction peaks were seen at 2θ values around 11.2° , 19.3° , and 22.5° , whereas for the binary solution-crystallized P(D-2HB)-0S, in addition to P(L-2HB)/PDLA HTSC crystalline diffraction peaks, the crystalline diffraction

peaks of the P(L-2HB) or P(D-2HB) homocrystallites and PDLA homocrystallites were observed at 2θ values around 14.7° and 16.8° , respectively.^{8–10,28–31} On the other hand, all of the ternary blends had the crystalline diffraction peaks in the 2θ values between those of P(L-2HB)/P(D-2HB) HMSC and P(L-2HB)/PDLA HTSC crystallites, that is, in the 2θ ranges of $10.7\text{--}11.3^\circ$, $18.5\text{--}19.6^\circ$, and $21.5\text{--}22.5^\circ$, although in addition to these peaks, P(D-2HB)-10S had the crystalline diffraction peaks of the P(L-2HB) or P(D-2HB) homocrystallites and PDLA homocrystallite at 2θ values around 14.7° and 16.8° , respectively.

The 2θ values of the blends in the ranges of $10.7\text{--}11.3^\circ$ and $21.5\text{--}22.5^\circ$, which are ascribed to the diffractions from (100/010/ -110) and (200/020/ -220) planes, respectively, in the case of poly(L-lactic acid)/PDLA HMSC,³² were monotonically increased with an increase in P(D-2HB) content, although the P(L-2HB)/PDLA HTSC crystalline diffraction peak position for the melt-crystallized blends with P(D-2HB) contents of 0–25 mol % at 2θ values around 11.3° remained unchanged, indicating the presence of P(L-2HB)/PDLA HTSC crystallites. In contrast, for the crystalline diffraction peaks in the 2θ range of $18.5\text{--}19.6^\circ$, it is difficult to see the change in 2θ , due to the overlapping of the peaks at around 18.6° and 19.3° for P(L-

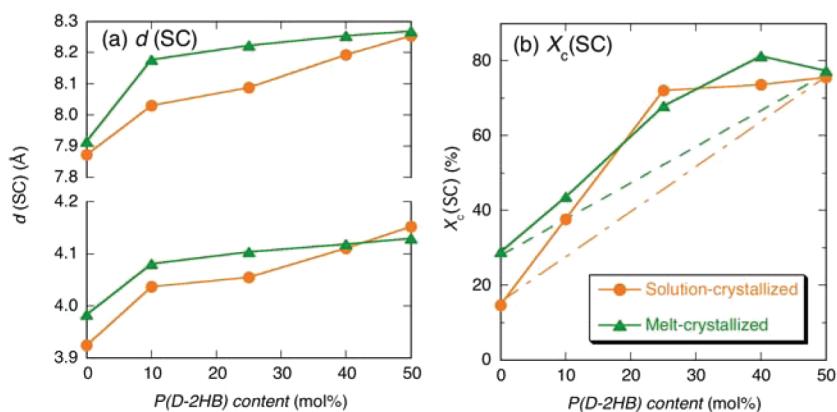


Figure 2. Interplane distance for 2θ values around 11° and 22° (upper and lower part data, respectively) (a) and crystallinity (b) of stereocomplex [$d(\text{SC})$ and $X_c(\text{SC})$, respectively] of solution- and melt crystallized blends as a function of P(D-2HB) content.

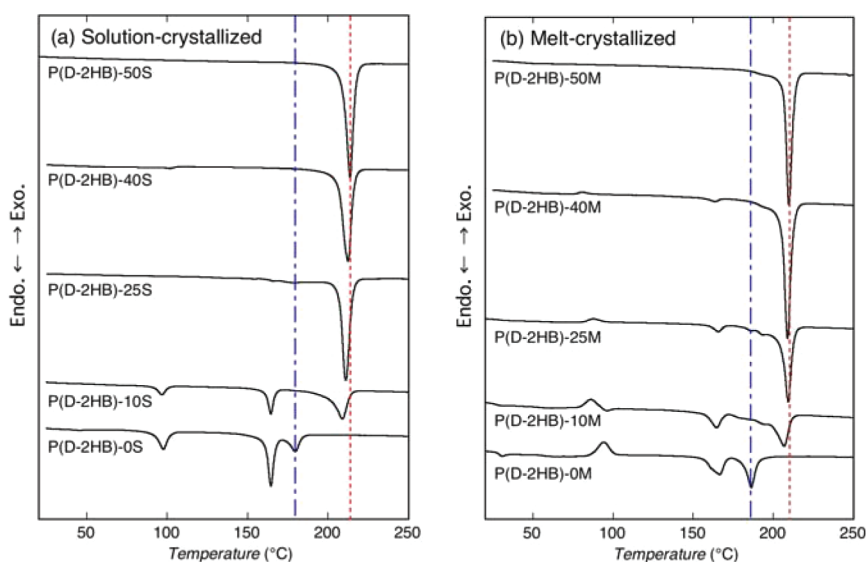


Figure 3. DSC thermograms of solution-crystallized (a) and melt-crystallized (b) blends. Red and blue lines are melting peaks of P(L-2HB)/P(D-2HB) HMSC and P(L-2HB)/PDLA HTSC crystallites, respectively.

2HB)/P(D-2HB) HMSC crystallites and that at around 19.3° for P(L-2HB)/PDLA HTSC crystallites.

The interplane distances of stereocomplex crystallites [$d(\text{SC})$ s] of the blends were estimated from P(D-2HB) content-sensitive crystalline diffraction peaks at 2θ values around 11° and 22° in Figure 1 and are plotted in Figure 2a as a function of P(D-2HB) content. As seen, both $d(\text{SC})$ values at 2θ values around 11° and 22° of solution- and melt-crystallized blends increased gradually with an increase in P(D-2HB) content. As the size of ethyl side chains of P(2HB) is larger than that of methyl side chains of PLA, the increases in $d(\text{SC})$ values with increasing P(D-2HB) content indicate the incorporation of P(D-2HB) chains into the P(L-2HB)/PDLA HTSC lattice or the incorporation of PDLA chains into the P(L-2HB)/P(D-2HB) HMSC lattice. In other words, the finding here indicates the ternary stereocomplex formation of L-configured P(L-2HB) and D-configured P(D-2HB) and PDLA in their ternary blends.

The X_c values for SC crystallites [$X_c(\text{SC})$] were evaluated from the WAXS profiles shown in Figure 1 and are plotted in Figure 2b as a function of P(D-2HB) content. The $X_c(\text{SC})$ values of HMSC at a P(D-2HB) content of 50 mol % were 76 and 77% for the solution- and melt-crystallized blends,

respectively, which were much higher than 15 and 29% of HTSC at P(D-2HB) content of 0 mol %. The $X_c(\text{SC})$ values of the blends increased rapidly with an increase in P(D-2HB) content up to 25 mol % and then saturated in the range of 70–80% for the P(D-2HB) content range of 25–50 mol %. The $X_c(\text{SC})$ values of the ternary blends were much higher than those calculated from $X_c(\text{SC})$ values of binary P(L-2HB)/PDLA HTSC and P(L-2HB)/P(D-2HB) HMSC crystallites at P(D-2HB) contents of 0 mol % and 50 mol %, respectively, assuming that HMSC and HTSC crystallites (not ternary stereocomplex) are separately formed without interaction between them. This finding also supports the formation of the ternary stereocomplex where relatively random incorporation or no strict selection of D-configured P(D-2HB) and PDLA is expected to occur during crystallization, in marked contrast with the separate crystallization into binary HMSC and HTSC crystallites, wherein D-configured P(D-2HB) and PDLA are strictly selected on their growth sites. This will result in higher $X_c(\text{SC})$ values of the ternary stereocomplex in the limited time of crystallization during solvent evaporation or isothermal annealing, in marked contrast with the case wherein both P(L-2HB)/P(D-2HB) HMSC and P(L-2HB)/PDLA HTSC crystallization separately takes place. Such rapid

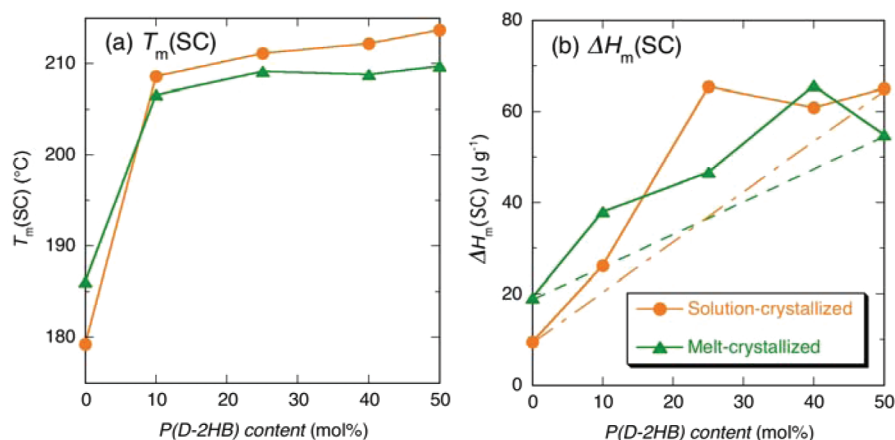


Figure 4. Melting temperature (a) and melting enthalpy (b) of stereocomplex [$T_m(\text{SC})$ and $\Delta H_m(\text{SC})$, respectively] of solution- and melt-crystallized blends as a function of P(D-2HB) content.

crystallization will facilitate the processing of high crystallinity materials with high heat-resistance in a short period of time.

To further investigate the thermal properties of ternary stereocomplex, DSC measurements were carried out for the blends, and their thermograms are shown in Figure 3. The endothermic peaks at around 100 and 170 °C are ascribed to the melting of P(L-2HB) or P(D-2HB) homocrystallites and PDLA homocrystallites, respectively, whereas those above 170 °C are attributed to the melting of stereocomplex crystallites.^{8,9} The T_m and ΔH_m of stereocomplex crystallites [$T_m(\text{SC})$ and $\Delta H_m(\text{SC})$, respectively] were estimated from the DSC thermograms shown in Figure 3 and are plotted in Figure 4 as a function of P(D-2HB) content. The $T_m(\text{SC})$ values of P(L-2HB)/PDLA HTSC crystallites in P(D-2HB)-0S and P(D-2HB)-0M were 179.2 °C and 186.1 °C, respectively, whereas those of P(L-2HB)/P(D-2HB) HMSC crystallites in P(D-2HB)-0S and P(D-2HB)-0M were 213.7 °C and 209.7 °C, respectively, which are higher than those of P(L-2HB)/PDLA HTSC crystallites (Figure 4a). The $T_m(\text{SC})$ increased rapidly with an increase in P(D-2HB) content in the range of 0–10 mol % and then slowly in the range of 10–50 mol %, indicating that the fraction of P(D-2HB) content in ternary stereocomplex crystallites increased with an increase in P(D-2HB) content in the blends. The $\Delta H_m(\text{SC})$ values (Figure 4b) showed the dependence on P(D-2HB) content similar to that of $X_c(\text{SC})$ (Figure 3b). The $\Delta H_m(\text{SC})$ values of the ternary stereocomplex were higher compared to those expected from the $\Delta H_m(\text{SC})$ values of binary stereocomplex crystallites, P(L-2HB)/PDLA HTSC and P(L-2HB)/P(D-2HB) HMSC crystallites at P(D-2HB) contents of 0 mol % and 50 mol %, respectively. This confirms the facile crystallization of ternary stereocomplex compared to the binary stereocomplexes, HMSC and HTSC, in the limited crystallization period of time. Finally, it should be stated that molecular weight and its distribution of the three polymers will affect the formation and crystallinity of the three types of stereocomplex crystallites.

In conclusion, this article first reports the ternary stereocomplex formation of L-configured P(L-2HB) and D-configured P(D-2HB) and PDLA, as evidenced by the findings that the $d(\text{SC})$ of the solution-cast and melt-crystallized ternary blends estimated from the 2θ values around 11° and 22° and the melting temperature of stereocomplex increased continuously with an increase in P(D-2HB) content relative to that of PDLA. The higher $X_c(\text{SC})$ and $\Delta H_m(\text{SC})$ values of the ternary blends

compared to those of the binary blends strongly suggested the relatively random incorporation or no strict selection of D-configured P(D-2HB) and PDLA, resulting in a higher crystallinity of the ternary stereocomplex in the limited crystallization period of time during solvent evaporation or isothermal treatment, in marked contrast with the case wherein both binary P(L-2HB)/P(D-2HB) HMSC and P(L-2HB)/PDLA HTSC crystallization separately occur.

EXPERIMENTAL SECTION

P(L-2HB) and P(D-2HB) were synthesized by the polycondensation of L- and D-2-hydroxybutanoic acids (L- and D-2-hydroxybutyric acids) ($\geq 97.0\%$, enantiomeric ratio $\geq 99:1$, Sigma-Aldrich Co.), respectively, with 5 wt % of *p*-toluenesulfonic acid (monohydrate, 99%, guaranteed grade, Nacalai Tesque, Inc., Kyoto, Japan) under a constant nitrogen gas flow at 130 °C at an atmospheric pressure for 5 h and then at a reduced pressure of 2.2 kPa for 18 h.^{7–10,33} PDLA was synthesized by the ring-opening polymerization of D-lactide (PURASORB D, Purac Biomaterials, Gorinchem, The Netherlands) in bulk at 140 °C initiated with 0.03 wt % of tin(II) 2-ethylhexanoate (Nacalai Tesque, Inc., Kyoto, Japan) in the presence of 0.6 wt % of D-lactic acid as co-initiators.³⁴ Tin(II) 2-ethylhexanoate was purified by distillation under reduced pressure before use. D-Lactic acid was prepared by hydrolytic degradation of D-lactide with water [D-lactide/water (mol/mol) = 1:2] at 100 °C for 30 min.³⁴ The synthesized P(L-2HB), P(D-2HB), and PDLA were purified by reprecipitation using chloroform and methanol as the solvent and nonsolvent, respectively, and then dried under reduced pressure for at least 7 days. The number-average molecular weight (M_n) and weight-average molecular weight (M_w)/ M_n of dried P(L-2HB), P(D-2HB), and PDLA were 1.42×10^4 g mol⁻¹, 1.26×10^4 g mol⁻¹, and 1.10×10^4 g mol⁻¹ and 1.50, 1.50, and 1.25, respectively, and their specific optical rotation values in chloroform at the wavelength of 589 nm and 25 °C and were -127 deg dm⁻¹ g⁻¹ cm³, 126 deg dm⁻¹ g⁻¹ cm³, and 152 deg dm⁻¹ g⁻¹ cm³, respectively, in agreement with the reported values.^{8,9}

Solution-crystallized blends were prepared by the procedure stated in previous papers.^{8,9} Briefly, each solution of two or three polymers was prepared separately to have a polymer concentration of 1.0 g dL⁻¹ and then admixed with each other under stirring. Dichloromethane was used as the solvent and the mixing ratios of P(L-2HB)/P(D-2HB)/PDLA were 50:0:50, 50:10:40, 50:25:25, 50:40:10, and 50:50:0 (mol/mol/mol). In these solutions, the fraction of L-configured P(L-2HB) was fixed at 50 mol %, and the content of D-configured P(D-2HB) relative to that of PDLA was varied. The solutions were cast onto Petri dishes, followed by solvent evaporation at 25 °C for approximately one day. For preparation of melt-crystallized blends, each solution-crystallized blend packed in a DSC aluminum pan was sealed in a test tube under reduced pressure, melted at 240 °C for 3 min,

crystallized at a predetermined crystallization temperature (T_c) = 160 °C for 10 h, and quenched at 0 °C for 5 min. The T_c of 160 °C was selected because the HTSC crystallization was confirmed to occur predominantly only at this temperature in an equimolar P(L-2HB)/PDLA blend.⁹

The M_w and M_n of the polymers were evaluated in chloroform at 40 °C with a Tosoh GPC system (refractive index monitor: RI-8020) with two TSK Gel columns (GMH_{XL}) using polystyrene standards. The T_m (SC) and ΔH_m (SC) of the blends were determined by a Shimadzu (Kyoto, Japan) DSC-50 differential scanning calorimeter with a cooling cover (LTC-50). The samples were heated from 0 to 250 °C at a rate of 10 °C min⁻¹ under a nitrogen gas flow of 50 mL min⁻¹ for DSC measurements. The T_m (SC) and ΔH_m (SC) values of the samples were calibrated using tin, indium, and benzophenone as standards.

The X_c (SC) values of the blends were estimated by the use of WAXS. The WAXS measurements were performed at 25 °C using a Rigaku (Tokyo, Japan) RINT-2500 equipped with a Cu K α source (λ = 0.1542 nm), which was operated at 40 kV and 200 mA. In a 2θ range of 7.5–25°, the crystalline diffraction peak areas for stereocomplex crystallites at 2θ values around 10.7–11.3°, 18.5–19.6°, and 21.5–22.5° relative to the total area between a diffraction profile and a baseline were used to estimate the X_c (SC) values.^{8–10,19,28–31}

AUTHOR INFORMATION

Corresponding Author

*E-mail: tsuji@ens.tut.ac.jp.

Notes

The authors declare no competing financial interest.

ACKNOWLEDGMENTS

This research was supported by a grant from Amano Institute of Technology, Japan.

REFERENCES

- (1) Slager, J.; Domb, A. J. *Adv. Drug Delivery Rev.* **2003**, *55*, 549–583.
- (2) Tsuji, H. *Macromol. Biosci.* **2005**, *5*, 569–597.
- (3) Fukushima, K.; Kimura, Y. *Polym. Int.* **2006**, *55*, 626–642.
- (4) Tsuji, H.; Ikada, Y. In *Biodegradable Polymer Blends from Renewable Resources*, Yu, L., Ed.; John Wiley & Sons, Inc.: Hoboken, NJ, 2009; p 165.
- (5) Grenier, D.; Prud'homme, R. E. *J. Polym. Sci., Polym. Phys. Ed.* **1984**, *22*, 577–587.
- (6) Voyer, R.; Prud'homme, R. E. *Eur. Polym. J.* **1989**, *25*, 365–369.
- (7) Ikada, Y.; Jamshidi, K.; Tsuji, H.; Hyon, S.-H. *Macromolecules* **1987**, *20*, 904–906.
- (8) Tsuji, H.; Okumura, A. *Macromolecules* **2009**, *42*, 7263–7266.
- (9) Tsuji, H.; Yamamoto, S.; Okumura, A.; Sugiura, Y. *Biomacromolecules* **2010**, *11*, 252–258.
- (10) Tsuji, H.; Shimizu, K.; Sakamoto, Y.; Okumura, A. *Polymer* **2011**, *52*, 1318–1325.
- (11) Tsuji, H.; Okumura, A. *Polym. J.* **2011**, *43*, 317–324.
- (12) Tsuji, H.; Tsuruno, T. *Macromol. Mater. Eng.* **2010**, *295*, 709–715.
- (13) Yui, N.; Dijkstra, P. J.; Feijen, J. *Makromol. Chem.* **1990**, *191*, 481–488.
- (14) Fukushima, K.; Hirata, M.; Kimura, Y. *Macromolecules* **2007**, *40*, 3049–3055.
- (15) Tsuji, H.; Wada, T.; Sakamoto, Y.; Sugiura, Y. *Polymer* **2010**, *51*, 4937–47.
- (16) Tsuji, H.; Ikada, Y.; Hyon, S. H.; Kimura, Y.; Kitao, T. *J. Appl. Polym. Sci.* **1994**, *51*, 337–344.
- (17) Takasaki, M.; Ito, H.; Kikutani, T. *J. Macromol. Sci., Phys.* **2003**, *42B* (3–4), 403–420.
- (18) Tsuji, H.; Ikada, Y. *Macromol. Chem. Phys.* **1996**, *197*, 3483–3499.
- (19) Zhang, J.; Tashiro, K.; Tsuji, H.; Domb, A. J. *Macromolecules* **2007**, *40*, 1049–1054.
- (20) Fujita, M.; Sawayanagi, T.; Abe, H.; Tanaka, T.; Iwata, T.; Ito, K.; Fujisawa, T.; Maeda, M. *Macromolecules* **2008**, *41*, 2852–2858.
- (21) Tsuji, H.; Nakano, M.; Hashimoto, M.; Takashima, K.; Katsura, S.; Mizuno, A. *Biomacromolecules* **2006**, *7*, 3316–3320.
- (22) Ishii, D.; Ying, T. H.; Mahara, A.; Murakami, S.; Yamaoka, T.; Lee, W.; Iwata, T. *Biomacromolecules* **2009**, *10*, 237–242.
- (23) Spasova, M.; Manolova, N.; Paneva, D.; Mincheva, R.; Dubois, P.; Rashkov, I.; Maximova, V.; Danchev, D. *Biomacromolecules* **2010**, *11*, 151–159.
- (24) Furuhashi, Y.; Yoshie, N. *Polym. Int.* **2012**, *6*, 301–306.
- (25) Purnama, P.; Kim, S. H. *Macromolecules* **2010**, *43*, 1137–1142.
- (26) Tsuji, H.; Yamamoto, S. *Macromol. Mater. Eng.* **2011**, *296*, 583–589.
- (27) Yang, C. F.; Huang, Y. F.; Ruan, J.; Su, A. C. *Macromolecules* **2012**, *45*, 872–878.
- (28) Pan, P.; Kai, W.; Zhu, B.; Dong, T.; Inoue, Y. *Macromolecules* **2007**, *40*, 6898–905.
- (29) Kawai, T.; Rahmann, N.; Matsuba, G.; Nishida, K.; Kanaya, T.; Nakano, M.; Okamoto, H.; Kawada, J.; Usuki, A.; Honma, N.; Nakajima, K.; Matsuda, M. *Macromolecules* **2007**, *40*, 9463–69.
- (30) Wasanasuk, K.; Tashiro, K. *Macromolecules* **2011**, *44*, 9650–9660.
- (31) Wasanasuk, K.; Tashiro, K.; Hanesaka, M.; Ohhara, T.; Kurihara, K.; Kuroki, R.; Tamada, T.; Ozeki, T.; Kanamoto, T. *Macromolecules* **2011**, *44*, 6441–6452.
- (32) Okihara, T.; Tsuji, M.; Kawaguchi, A.; Katayama, K.; Tsuji, H.; Hyon, S.-H.; Ikada, Y. *J. Macromol. Sci., Phys.* **1991**, *B30*, 119–140.
- (33) Tsuji, H.; Matsuoaka, H.; Itsuno, S. *J. Appl. Polym. Sci.* **2008**, *110*, 3954–3962.
- (34) Tsuji, H.; Sugiura, Y.; Sakamoto, Y.; Bouapao, L.; Itsuno, S. *Polymer* **2008**, *49*, 1385–1397.